Influence of titanium carbide addition on densification and microstructure of alumina ceramics doped with niobium oxide and lithium fluoride

Pedro Henrique Poubel Mendonça da Silveira[a,b], Matheus Pereira Ribeiro[a], Thuane Teixeira da Silva[a], Pedro Craveiro Rodrigues dos Santos Credmann[a], Paulo Roberto Rodrigues de Jesus[a], Alaelson Vieira Gomes[a]

[a]Seção de Engenharia de Materiais SE/8, Instituto Militar de Engenharia. [b]pedroo.poubel@gmail.com

RESUMO: Compósitos de matriz cerâmica são objetos de estudo no setor balístico por conta da alta dureza associada a tenacidade à fratura e melhoria na performance balística em sistemas de blindagem multicamadas. As cerâmicas sem a presença de dopantes dificultam o processamento e podem comprometer as propriedades finais do material sinterizado. Este trabalho visou o processamento cerâmico de compósitos de matriz cerâmica à base de Al_2O_3, com adições de 4 %p de Nb_2O_5, 0,5 %p de LiF e 38,5 %p de TiC, processados por sinterização convencional a 1400 °C/1h. As cerâmicas sem a presença de TiC apresentaram altos valores de densificação, já as amostras com adições de TiC tiveram reduções severas em sua densificação, tornando- se tornando um material extremamente frágil e quebradiço.

PALAVRAS-CHAVE: Compósitos de Matriz Cerâmica; Microestrutura; Sinterização; Alumina; Carbeto de Titânio.

ABSTRACT: Ceramic matrix composites are objects of study in the ballistic sector due to the high hardness associated with fracture toughness and improved ballistic performance in multilayer shielding systems. Ceramics without the presence of dopants make processing difficult and may compromise the final properties of the sintered material. This work aimed at the ceramic processing of ceramic matrix composites based on Al_2O_3, with additions of 4 w% of Nb_2O_5, 0.5 wt% of LiF and 38.5 wt% of TiC, processed by conventional sintering at 1400 °C/1h. Ceramics without the presence of TiC showed high densification values, whereas samples with TiC additions had severe reductions in their densification, becoming an extremely fragile and brittle material.

KEYWORDS: Ceramic Matrix Composites; Microstructure; Sintering; Alumina; Titanium Carbide.

1. Introduction

The need for the use of composite materials has been growing due to their high weight stability, high strength and relatively low density when compared to other classes of materials. Therefore, composites have been used in industries such as aerospace, automotive, military and many other fields in recent decades. One of the main applications of composites is ballistic protection, which uses this class of materials in the military field. Thanks to their low weight, composites are preferred for the construction of aircraft, tanks and bulletproof vests [1].

The ceramic materials used in ballistic armor must have a sufficient degree of fragmentation of the bullet, in addition to reducing its speed, transforming it into small fragments that must be covered by the posterior layer of the armor, consisting of flexible material that supports the ceramic. Therefore, it is necessary that the ceramic material has a high modulus of elasticity, in addition to high hardness and good fracture toughness [2-4].

The main ceramic materials used commercially in the development of ballistic armor are Al_2O_3, B_4C, SiC and ceramic matrix composites (CMCs), such as the Al_2O_3/ZrO_2 system or $Al_2O_3/Nb_2O_5/LiF$. The high cost, combined with processing restrictions and difficulties in predicting the ballistic performance of the properties of these materials, are setbacks for ceramic mechanisms, requiring the inclusion of other elements to improve properties and reduce costs [5-8].

In this way, Al_2O_3 provides the best cost-benefit ratio among advanced ceramics, featuring a high modulus of elasticity, high performance as a refractory, high hardness and relatively lower cost. However, due to its low fracture toughness and low flexural strength, the ballistic performance of alumina is lower when compared to SiC and to B4C [1,3,9].

One factor to be taken into account in the processing of ceramics for ballistic armor is the formation of a liquid phase. This phase provides the material with greater densification, accompanied by a reduction in the sintering temperatures of the materials, without loss of properties. An example is the use of niobium (Nb2O5), where its addition to alumina in amounts from 1 to 8% by weight provides a considerable reduction in the sintering temperature in alumina [10,11].

Another important factor is the addition of carbides to the ceramic matrix. Additions of this group of ceramics in the matrix of Al_2O_3 (such as NbC, SiC, B_4C), allows an increase in hardness and fracture toughness [12]. In the development of CMCs for shielding, a material with good properties used as an interstitial addition to provide greater hardness and fracture toughness is titanium carbide (TiC) [12-16].

TiC is an extremely hard ceramic (Mohs hardness 9 - 9.5) and has an extremely high melting point (3260 °C) [12-16]. However, the processing of CMCs made up of Al2O3-TiC is difficult since techniques such as plasma sintering (SPS) or hot pressing (HP) are required. From these techniques, it is possible to obtain a faster sintering, and with densities around 95% of the DT, but they are techniques of difficult availability [16].

Aiming at a simpler and cheaper processing, the objective of this work is to process through conventional sintering and cold isostatic pressing Al_2O_3 matrix, CMCs, with additions of TiC and the use of Nb_2O_5 and LiF as sintering additives.

2. Methodology

2.1 Starting Materials

The powders used for the manufacture of ceramic bodies are: α-Al_2O_3 acquired at Treibacher Schleifmittel (Brazil), with an average grain size of 3 μm, the Nb_2O_5 was acquired by Companhia Brasileira de Metalurgia e Mineração (Brazil), the lithium fluoride (LiF) used was obtained by Vetec (Brazil), the TiC used in the addition was acquired from the company Sigma Aldrich (USA), and the organic binder used to confer resistance to the body to green is Polyethylene glycol (PEG 300) from the company Isofar (Brazil). Next, in **table** 1, the materials used in the manufacture of ceramic compounds and the densities of each component used are described.

Tab. 1 - Density of the constituent elements of the ceramics produced.

Material	Density (g/cm³)
Al_2O_3	3,98
Nb_2O_5	4,60
LiF	2,60
TiC	4,93
PEG 300	--

The density of the mixtures was determined from the Rule of Mixtures, given below in **equation** 1, where the densities of each element of the mixture and their fraction by weight were used, excluding the PEG that is eliminated during sintering.

$$\rho = (\rho_A \times m_A) + (\rho_B \times m_B) \qquad (1)$$

The percentages of addition of each element were 0.5% by weight of LiF, 4% by weight of Nb_2O_5 and 38.5% by weight of TiC. In **table** 2, the densities of each mixture composition are described.

Tab. 2 - Theoretical density of the samples obtained using the mixture rule.

Material	Density (g/cm³)
Al_2O_3-Nb_2O_5	4,00
Al_2O_3-Nb_2O_5-LiF	3,99
Al_2O_3-TiC-Nb_2O_5	4,37
Al_2O_3-TiC-Nb_2O_5-LiF	4,36

2.2 Sample Processing

The starting materials were placed in an alumina-lined jar. Along with these elements, deionized water was inserted in a 1:1 ratio to facilitate homogenization, and alumina balls for better comminution of the powders. Grinding and mixing was done in a ball mill for a period of 8 hours, followed by drying in an oven at a temperature of 80°C for a period of 48 hours.

After drying, the mixture resulting from the milling was deagglomerated with the aid of a pestle and mortar, followed by sieving to obtain the desired granulometry. A sieve shaker was used for a period of 3 min using a DIN 4188 sieve with an opening of 0.255 mm.

The preparation of the green ceramic bodies was done through uniaxial cold pressing, using a SKAY press, with a capacity of 30 t. Ceramic disks were prepared with 20 mm diameter matrices for the Archimedes tests and pressed in two stages: the first stage consisted of a pre-load of 15 MPa for the settlement of the powders in the matrix for a period of 30 s, the second stage consisted of pressing with a load of 50 MPa to give the powders a tablet shape.

The sintering of the samples was done in a conventional way, without the presence of a controlled atmosphere. Sintering was carried out in a JUNG furnace with the process reaching a maximum temperature of 1400 °C. The sintering route is shown below in **figure** 1.

Fig. 1 – Sintering route used in this study.
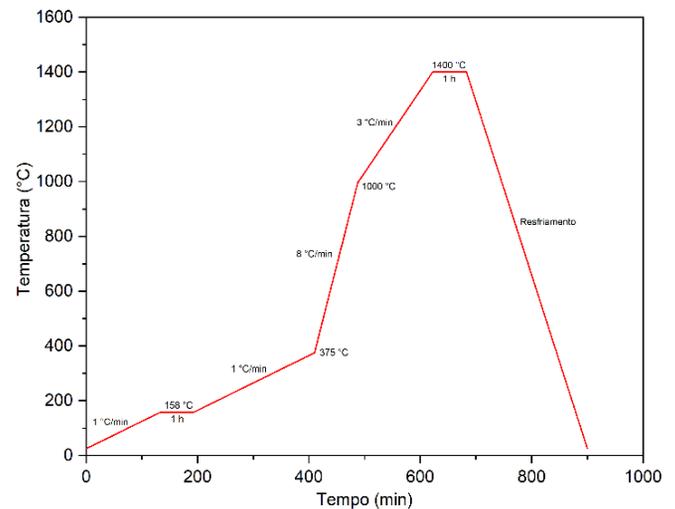
2.3 Characterization
2.3.1 Green Densification Calculation

From the theoretical density value found through the Rule of Mixtures, it was possible to calculate the density and densification of the green ceramic bodies.

Equation 2 was used to determine the density of the bodies in green through the difference between the mass and the volume of the sample.

The densification in green, shown below in **equation** 3, was calculated based on the percentage difference in the density value obtained by the theoretical density found in the mixture rule of **equation** 1.

$$\rho_{greeen} = \frac{mass_{sample}}{volume_{sample}} \quad (2)$$

$$Densification = \left(\frac{\rho_{apparent}}{\rho_{theoretical}}\right) \times 100\% \quad (3)$$

2.3.2 Densification of Sintered Samples

The calculation of density and densification of the sintered ceramic bodies was performed based on NBR 16667: 2017. [15] The calculation is carried out based on the Archimedes technique, where the data obtained from

the immersed mass (mi) is used, wet mass (mu) and dry mass (ms) to determine the apparent density through **equation** 4, and with this result determine the densification of the ceramic body through the difference between the apparent density and the theoretical density of the body (**equation** 5).

$$\rho_{apparent} = \left(\frac{m_s}{m_u - m_i}\right) x \, \rho_{liq} \qquad (4)$$

$$Densification = \left(\frac{\rho_{apparent}}{\rho_{theoretical}}\right) x \, 100\% \qquad (5)$$

2.3.3 Scanning Electron Microscopy (SEM)

Fracture surface analysis of the sintered samples was performed using a QUANTA FEG 250 scanning electron microscope. Beam power of 5kV, 20kV and 25kV was used, beam diameter 5.5 μm and magnification of 500x and 2000x to observe the microstructures. The samples were covered with gold to enable visualization on SEM.

3. Results and Discussion

3.1 Green Densification

Below in Table 3, the density and densification values in green for the four groups of samples before sintering are presented.

Tab. 3 - Density and densification in green of the bodies in green.

Samples	Density (g/cm³)	Densification (%)
Al_2O_3-Nb_2O_5	2,02 ± 0,01	50,64 ± 0,44
Al_2O_3-Nb_2O_5-LiF	2,12 ± 0,10	53,37 ± 2,57
Al_2O_3-TiC-Nb_2O_5	1,48 ± 0,05	33,86 ± 1,21
Al_2O_3-TiC-Nb_2O_5-LiF	1,44 ± 0,10	33,11 ± 2,31

From the values displayed in **table** 3, it is observed that the samples without addition of TiC presented satisfactory green densification values. For ceramics to achieve good densification after sintering, it is necessary to have a densification of the green bodies of approximately 55% of the theoretical density or higher. Samples with TiC additions showed very low densification values, which results in low densification of the bodies after sintering. Another factor to be taken into account was the difficulty in securing the bodies with the addition of TiC, as they had lamination and endcapping defects.

3.2 Densification of Sintered Samples

Next, in **table** 4, the density and densification values of the sintered samples are shown.

Tab. 4 - Density and green densification of sintered samples.

Samples	Density (g/cm³)	Density (%)
Al_2O_3-Nb_2O_5	3,39 ± 0,07	84,88 ± 1,77
Al_2O_3-Nb_2O_5-LiF	3,69 ± 0,02	92,71 ± 0,50
Al_2O_3-TiC-Nb_2O_5	1,06 ± 0,01	24,22 ± 0,26
Al_2O_3-TiC-Nb_2O_5-LiF	9,99 ± 0,01	29,19 ± 0,58

The mean densification values of the groups were very different from each other. The group samples Al_2O_3/Nb_2O_5/LiF presented the highest densification of all groups, with values close to those obtained in the literature, above 91% [5,6,11]. Meanwhile, the samples from the group Al_2O_3/Nb_2O_5, showed a lower value, with densification close to 85%, this is due to the fact that only the $AlNbO_4$ phase was formed during homogenization. [18] The group with LiF, on the other hand, presents interaction of this element with Nb_2O_5, fcausing the $LiNbO_3$ and Nb_3O_7F dphases to occur during sintering.

On the other hand, the two groups with the presence of TiC in the composition showed severe reductions in the densification of the samples (values less than 30%). This low densification may be a result of

the high TiC content used in the composition (38.5% by weight), preventing the material from becoming lodged as an interstitial element in the alumina.

It is possible to assume from data in the literature that, without the presence of an inert atmosphere, TiC reacts with oxygen, forming the titanium (TiO_2) phase, which could even favor sintering in the presence of a liquid phase. [15,16] However, its excessively high concentration, combined with the low densification of the ceramic disks during pressing, may have impaired the interaction of the samples, causing the result to be porous and brittle disks..

3.3 Microstructure of Sintered Samples

Next, in **figures** 2 and 3, the images obtained with the aid of SEM of the fracture surface of the sintered samples are contained.

Fig. 2 – Micrographs of the fracture regions of the sintered samples at 500x magnification: (a) Al_2O_3/Nb_2O5; (b) $Al_2O_3/Nb_2O_5/LiF$; (c) $Al_2O_3/TiC/Nb_2O_5$; (d) $Al_2O_3/TiC/Nb_2O_5/LiF$.
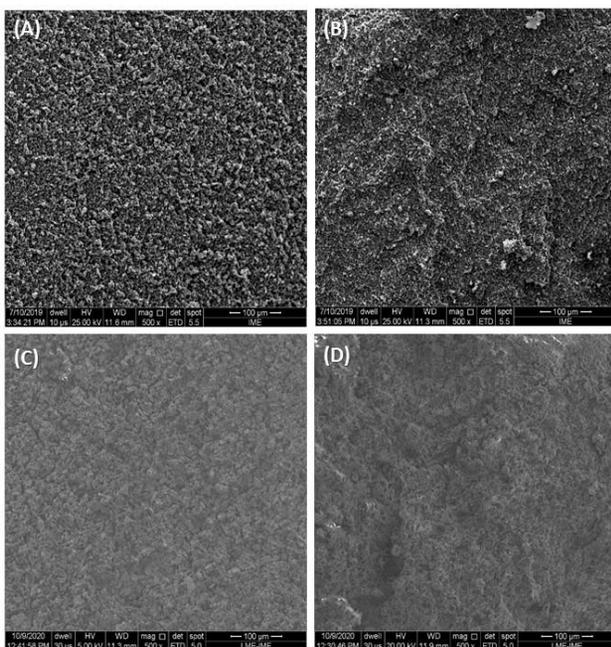
The micrographs in **figure** 2 generally show the fracture region of the sintered samples. As can be seen, the samples from the groups Al_2O_3/Nb_2O_5 and $Al_2O_3/Nb_2O_5/LiF$ they have less porosity on their surface, as a

result of the high densification obtained in the sintering of these two groups.

The samples with addition of TiC in the composition showed high porosity on their surface, resulting from the low interaction of the grains during sintering. During the coating of samples for SEM analysis, there was difficulty in deposition of gold in samples with TiC, as part of this material is deposited in the pores, escaping from the surface. Thus, during the analysis, it was not possible to generate the images of these two groups with the same power of the electron beam (25kV), making it necessary to reduce the power of the beam to 5kV for the analysis of the sample of the group $Al_2O_3/TiC/Nb2O5$ due to the excess of light loading in the image, and 20kV power for the sample of the group containing $Al_2O_3/TiC/Nb_2O_5/LiF$.

Next, in **figure** 3, the micrographs with 2000x magnification are present, with a better visualization of the morphology of the grains

Fig. 3 – Micrographs of the fracture regions of the sintered samples at 500x magnification: (a) Al_2O_3/Nb_2O_5; (b) $Al_2O_3/Nb_2O_5/LiF$; (c) $Al_2O_3/TiC/Nb_2O_5$; (d) $Al_2O_3/TiC/Nb_2O_5/LiF$.
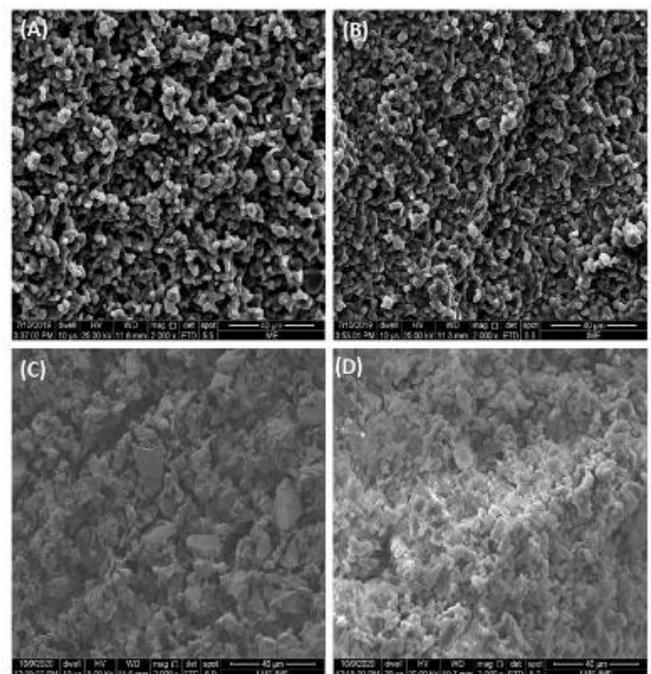
The micrographs in **figure** 3 show the morphology of the grains in more detail. The samples of the groups Al_2O_3/Nb_2O_5 and $Al_2O_3/Nb_2O_5/LiF$ have rounded grains, in addition to the formation of well-defined necks, the result of good compaction and sintering. There is also the presence of pores, however these pores are small and well distributed throughout the samples, resulting from the good wetting of the liquid phase during sintering.

The samples of the two groups with addition of TiC ($Al_2O_3/TiC/Nb_2O_5$ and $Al_2O_3/TiC/Nb_2O_5/LiF$) showed a large amount of pores, in addition to grains with different dimensions. This could have happened due to poor homogenization during milling, followed by difficulty in compacting the samples and sintering that caused impoverishment of the samples.

4. Conclusions

In this work, four different groups of ceramic matrix composites were produced by uniaxial cold pressing and conventional sintering, and characterized by Archimedes test and SEM. From the collected results, it is possible to conclude that the samples with additions of TiC showed low density in green, which means that the pressure of 50 MPa was not enough for a good densification of the bodies in green. Samples with TiC showed extremely low densification, making it even difficult to cover them with conductive material for SEM analysis, requiring a variation in the intensity of the electron beam to perform the analysis.

The samples without the addition of TiC showed high values of density in green and after sintering, as previously obtained in other works, showing that sintering without the presence of TiC was satisfactory.

Acknowledgements

References

[1] B. Tepeduzu, R. Karakuzu. Ballistic performance of ceramic/composite structures, Ceramics International, 2019, 45(2), pgs 1651-1660.

[2] Yadav, S. and Ravichandran, G., 2003. Penetration resistance of laminated ceramic/polymer structures. International Journal of Impact Engineering, 28(5), pp.557-574.

[3] Silva, M., Stainer, D., Al-Qureshi, H., Montedo, O. and Hotza, D., 2014. Alumina-Based Ceramics for Armor Application: Mechanical Characterization and Ballistic Testing. Journal of Ceramics, 2014, pp.1-6.

[4] Karandikar, P., Evans, G., Wong, S., Aghajanian, M. and Sennett, M., n.d. A Review of Ceramics for Armor Applications. Ceramic Engineering and Science Proceedings, 29(6), pp.163-175.

[5] Santos, J., Marçal, R., Jesus, P., Gomes, A., Lima, E., Monteiro, S., de Campos, J. and Louro, L., 2017. Effect of LiF as Sintering Agent on the Densification and Phase Formation in Al2O3-4 Wt Pct Nb2O5 Ceramic Compound. Metallurgical and Materials Transactions A, 48(10), pp.4432-4440.

[6] Santos, J., Marçal, R., Jesus, P., Gomes, A., Lima, É., Navarro da Rocha, D., Santos, M., Nascimento, L., Monteiro, S. and Louro, L., 2018. Mechanical properties and ballistic behavior of LiF-added Al2O3–4 wt%Nb2O5 ceramics. Journal of Materials Research and Technology, 7(4), pp.592-597.

[7] Seong, W., Ahn, B., Min, Y., Hwang, G., Choi, J., Choi, J., Hahn, B., Cho, Y. and Ahn, C., 2020. Effect of Nb2O5 addition on microstructure and thermal/mechanical properties in zirconia-toughened alumina sintered at low temperature. Ceramics International, 46(15), pp.23820-23827.

[8] Huang, C. and Chen, Y., 2016. Effect of mechanical properties on the ballistic resistance capability of Al 2 O 3 -ZrO 2 functionally graded materials. Ceramics International, 42(11), pp.12946-12955.

[9] Fabris, D., Polla, M., Acordi, J., Luza, A., Bernardin, A., De Noni, A. and Montedo, O., 2020. Effect of MgO·Al2O3·SiO2 glass-ceramic as sintering aid on properties of alumina armors. Materials Science and Engineering: A, 781, p.139237.

[10] Cabral, R., Prado da Silva, M., de Campos, J. and Lima, E., 2012. Study of the Sintering of Mixtures Al2O3--Nb2O5 and Y2O3-Nb2O5. Materials Science Forum, 727-728, pp.799-803.

[11] Silveira, P., Jesus, P., Ribeiro, M., Monteiro, S., Oliveira, J., Gomes, A., 2020. Sintering Behavior of Al2O3 Ceramics Doped with Pre-Sintered Nb2O5 and LiF. Materials Science Forum, 1012, pp.190-195.

[12] Fu, Z. and Koc, R., 2017. Pressureless sintering of submicron titanium carbide powders. Ceramics International, 43(18), pp.17233-17237.

[13] Compton, B. and Zok, F., 2013. Impact resistance of TiC-based cermets. International Journal of Impact Engineering, 62, pp.75-87.

[14] Cheng, L., Xie, Z., Liu, G., Liu, W. and Xue, W., 2012. Densification and mechanical properties of TiC by SPS--effects of holding time, sintering temperature and pressure condition. Journal of the European Ceramic Society, 32(12), pp.3399-3406.

[15] Koc, R. and Folmer, J., 1997. Carbothermal Synthesis of Titanium Carbide Using Ultrafine Titania Powders. Journal of Materials Science, 32(12), pp.3101-3111.

[16] Koc, R., 1997. Kinetics and phase evolution during carbothermal synthesis of titanium carbide from carbon--coated titania powder. Journal of the European Ceramic Society, 17(11), pp.1309-1315.

[17] NBR 16661:2017. Material refratário denso conformado – determinação de volume aparente, volume aparente da parte sólida, densidade da massa aparente, densidade aparente da parte sólida, porosidade aparente e absorção. ABNT. 2ª edição; 2017.

[18] Kong, F., Lv, L., Wang, J., Jiao, G., Tao, S., Han, Z., Fang, Y., Qian, B. and Jiang, X., 2018. Graphite modified AlNbO 4 with enhanced lithium — Ion storage behaviors and its electrochemical mechanism. Materials Research Bulletin, 97, pp.405-410.

[19] Huang, F., Zhao, H., Yan, A., Li, Z., Liang, H., Gao, Q. and Qiang, Y., 2017. In situ thermal decomposition for preparation of Nb3O7F/Nb2O5 hybrid nanomaterials with enhanced photocatalytic performance. Journal of Alloys and Compounds, 695, pp.489-495.